IMPLEMENTATION OF TECHNICAL SPECIFICATIONS TO STANDARDISE AND IMPROVE ELECTROLUMINESCENCE IMAGING TEST SETUPS

Jacqui Crozier McCleland[1], Isaac Kwembur[2], Ross Dix-Peek[3], Frederik Vorster[4], E Ernest van Dyk[5]

[1]Department of Physics, PO Box 77000, Nelson Mandela University, Port Elizabeth 6031, South Africa

*Corresponding Author: email: jcrozier@mandela.ac.za; Tel: 041 5042856; Fax: 041 5041755

[2] Nelson Mandela University; s218207115@mandela.ac.za
[3] Nelson Mandela University; s212286552@mandela.ac.za
[4] Nelson Mandela University; Frederik.vorster@mandela.ac.za
[5]Nelson Mandela University; Ernest.vanDyk@mandela.ac.za

Abstract

Electroluminescence (EL) is an important tool in photovoltaic (PV) module quality testing and module degradation assessment. EL imaging is primarily a qualitative test that allows for cell cracks and severe damage to be easily identified. Degradation occurs over the lifetime of a module, so it is essential that EL images are recorded in a way that is consistent and comparable to ensure that the degradation is reliably monitored. In order to be able to compare images taken at different labs and over a period of years, the test procedure needs to standardised to ensure that results are comparable. This paper sets out the best practices for lab EL imaging of modules and on-site imaging informed by the Technical Specification (IEC TS 60904-13:2018) and current research. The quality of the EL imaging results is dependant on the camera used, the test setup factors such as camera position, number of images per module and light conditions. Optimum camera focus is essential for sharp images and a procedure to assist manual focusing is suggested. Five test setups for modules, cells and module-strings are compared, either involving a single camera/image setup or multiple images/cameras. The resolution and sharpness are compared for each setup. The additional cost and/or time involved in the better image resolution needs to be weighed up to the importance of detecting finer defects. If the requirement is to detect major defects then faster, cheaper systems can be used but in order to detect fine cracks and defects the additional cameras or longer testing times are needed.

Keywords: Electroluminescence; Module Degradation; Image Processing.

1. Introduction

1.1. Electroluminescence

Electroluminescence (EL) imaging has developed from a lab-based techniques [1] to an essential part of the quality testing of PV modules, integrated into the manufacturing process, installation, and the ongoing monitoring of module degradation [2][3]. This involves forward biasing the module by up to Short-circuit Current (Isc) and detecting the emitted luminescence. The areas of poor electrical contact due to cracks or damage will be appear darker than the other cells in the module. This requires low light conditions, a camera with appropriate filters and a power supply capable of supplying the required bias [1][4]. EL imaging has evolved and has been informed by ongoing research, culminating in the publishing of an IEC Technical Specification IEC TS60904-13:2018 [5], which sets out the requirements for imaging and quantitative and qualitative evaluation.

This paper sets out the best practices for lab EL Imaging of modules and on-site Imaging informed by the Technical Specification and current research. Degradation occurs over the lifetime of a module, so it is essential that EL images are recorded in a way that is consistent and comparable to ensure that the degradation is reliably monitored.

EL images obtained from different laboratory test setups are compared, the setups vary based on camera position, number of cameras and image processing procedure. All the test setups are optimised to achieve ideal focus, sharpness and signal to noise ratio (SNR) according to IEC TS 60904-13:2018[5]. On-site EL images are also compared to lab-based imaging, as a potential technique for identifying major defects in the field.

1.2. Camera Settings

1.2.1. Camera, Filters and Lenses

For EL imaging a silicon charge-coupled device (CCD) camera was used because it has very good spatial resolution however this sensor is only sensitive to wavelength in the range of 300-1200 nm. There is an overlap in wavelengths from about 900 to 1100 nm allowing the EL emitted from silicon solar cells to be detected [1]. NIR sCMOS also overlaps a sufficient portion of the EL emission spectrum to be used for EL imaging, and they are typically less expensive [3]. The lenses used must be free of absorption filters or coatings and can be used to cut extraneous wavelengths [5].

1.2.2. ISO or Gain

ISO value is a measure of the sensitivity of the image sensor [3]. It is the amplification level between the pixel photon created charge and the pixel brightness, so the higher the ISO value the greater the sensor's light sensitivity. The ISO setting affects the Signal to Noise ratio and should be kept constant.

1.2.3. Aperture Value (f-stop)

The aperture range of a lens refers to the amount that the lens can open or close, to let in more or less light, respectively. Apertures are listed in terms of f-numbers, which quantitatively describe relative light-gathering area. The f-stop is f/2.8 for all EL setups described in this paper. This smaller aperture size means the shutter speed is slower (longer exposure time) and increases the depth of field.

1.2.4. Environmental Conditions

EL images can be done in low-light or dark conditions depending on the camera and filters. NIR CMOS cameras require a completely dark environment. By subtracting a background image it is possible to use some cameras in low light conditions

Temperature has an proven effect on the EL intensity [6], however, for the purposes of qualitative EL imaging the effect is not significant. The lab temperature should be maintained in the range of 20-25°C and noted at the time of test. With on-site imaging no temperature control is possible but considering the low resolution of the images this is not a concern.

1.2.5. Bias Levels

EL intensity has a strong dependence on the applied bias[7]. For the purposes of quality assessment, the EL images are only captured at the following levels:

- 110% Isc
- 100% Isc
- 10% Isc
- 0 – Background

110%Isc is not specified by IEC TS 60904-13:2018[5] but can be requested by clients. 10%Isc allows for the detection of Potential Induced Degradation Imaging (PID) [8].

The applied bias is only measured by the power supply, this contributes to uncertainty but for the purpose quanlitative EL it is sufficient. This level should be noted for every EL image. The current is set in the power supply and the voltage is set at 120% of the modules open-circuit voltage to ensure that the required current is reached.

2. Experimental Procedure

2.1. EL setups

The EL Setup consists of the following components: a Camera, with appropriate lenses and filters, a Dark room/low light environment, an appropriate power supply and appropriate structure to hold the module and camera such the optical axis of the camera shall be placed perpendicularly and as close as possible to the module face to image the solar cell or module area [5]. Positioning the camera directly in front of the module is easy in lab test but is not possible in onsite test and thus onsite EL image requires some image correction.

The five test setups are that are compare in this paper are detailed in Table 1. Setups A and D consist of a single camera positioned on a tripod, with a working distance such that the entire module is captured in a single image.

Setup B involves multiple cameras in a dark box and the module is mounted on a linear axis tray and moved in front of the cameras in order to capture the entire module in 12 images. In setup D, the module is mounted above the camera in dark box and an X-Y stage moves the camera from one cell to the next [4] and captures an image for every cell in the module. This is the most time consuming EL setup. In Setup C, the camera mounted over the module in a dark room and then is manually moved to capture the entire module in two images.

Setup E is for Onsite testing of module-strings without disconnecting or removing them from the racks. The camera is mounted on a tripod and positioned such that an entire string can be imaged. The amount of images required per string depends on the array layout and the level of detail required.

The cameras in setup A and E are equipped with appropriate filters that allow the imaging to be done in low light conditions in the lab so imaging can be done in low light conditions from dusk onwards. The cameras in setups B, C and D require no stray light and imaging must be done in dark room or box. Cameras B/C are CMOS cameras while the rest are CCD.

EL Setup	A	B	C	D	E
Level	Module	Module	Module	Cell	Module String
Camera Detector	CCD sensor	CMOS	CMOS	CCD sensor	CCD sensor
# Cameras	1	4	1	1	1
Images per module	1	12	2	Each Cell	Multiple Modules
Camera Resolution (H x V pixels)	1024 x1024	2048 x 1536	2048 x 1536	3324 x 2504	1024 x1024
Light Conditions	Low Light	Dark Room	Dark room	Dark room	Low light

Table 1: A Summary of the EL setups described in this paper.

2.2. Camera Settings

2.2.1. Resolution

The image resolution is an important factor in the overall image quality and is determined by the camera used and the setup design. In order to maximise the resolution of an EL image, the camera sensor resolution can be increased or smaller portions of the module can be captured in each image, decreasing the Field of View (FOV)[5].

$$\textit{Sensor resolution} = \textit{Image resolution} = \textit{FOV/smallest image feature} \quad 1.1.$$

Within the confines of the camera used and test setup, the maximum resolution and pixel size is given in Table 2.

2.2.2. Focus

All the cameras used have manual focussing and thus the focus must be checked and locked when there are any changes in the setup positions. Setup B cameras are in a static position so focus can be checked as part of annual maintenance.

Manual focusing of camera requires the subjective assessment of the images in order to make sure the image is clear. Alternatively, the focus can be quantified and compared in the method described in the standard [5][9] and using image processing software [10].

2.2.3. Image Signal-to-Noise Ratio (SNR)

The signal to noise ratio (SNR) is defined as

$$SNR = \frac{N_s}{u} \quad 1.2$$

Where N_s is equal to the number of generated signal electrons and *u* is the standard deviation of the mean. The signal to noise ratio and sources of noise are important when making qualitative assumptions from EL images [11]. The parameters of the camera are set in order to obtain an EL image with the highest possible signal to noise ratio.

The sources of noise are [12]:

- Photon Noise, σ_s , due to the variation of emitted photons with time.
- Dark Noise, σ_{drk}, thermal stimulation generates electrons within the CCD sensor these are minimised by cooling the sensor.
- Readout Noise, σ_{ro}, occurring due to the readout electronics themselves due to the amplification of the signal and the conversion into a voltage.
- Cooling Fluctuations, σ_{ro}, are due to inconsistencies in the cooling of the sensor can contribute to additional noise however this is less significant in Si cameras because the sensor is strongly cooled and has a large band-gap.

The background image can be subtracted from the EL image in order to remove the effects of stray light and dark current though it does increase the noise present in the image. The total noise can be determined by adding the variance of each source. Since the dark noise, readout noise and cooling noise is present in both the dark background and the EL image these variances are included twice in the total. This holds for a CCD camera such as camera D which does not have electron multiplier gain[12].

Determining the signal to noise ratio of an EL imaging setup has been included in the IEC TS 60904-13:2018 because it affects the image quality and in turn the ability to identify the features in the image. The SNR would be different at each Bias level and exposure time but can be calculated for a reference module and then result can be inferred to other modules, the gain or ISO settings are not changed[5].

2.2.4. Exposure Time

The exposure time is adjusted to achieve optimum SNR while not ensure that it does not create overexposed areas or saturated areas of the image. The exposure time depends on the bias level and should be adjusted so that the image has a distributed signal intensity. The optimum exposure time varies with each setup.

2.3. Image Processing

In order to compare images and give a measure of degradation, the image processing procedure should be consistent in order to compare images. Image processing can include cropping the image to include only the active area, background image subtractions and level range adjustment.

3. Results

3.1. EL images

Figure 1 shows an EL image of a module in each of the setups that image at a module level. In all images significant cell breakages would be visible, however, in setup B and C finer

module details such as the grid fingers and microcracks are visible.

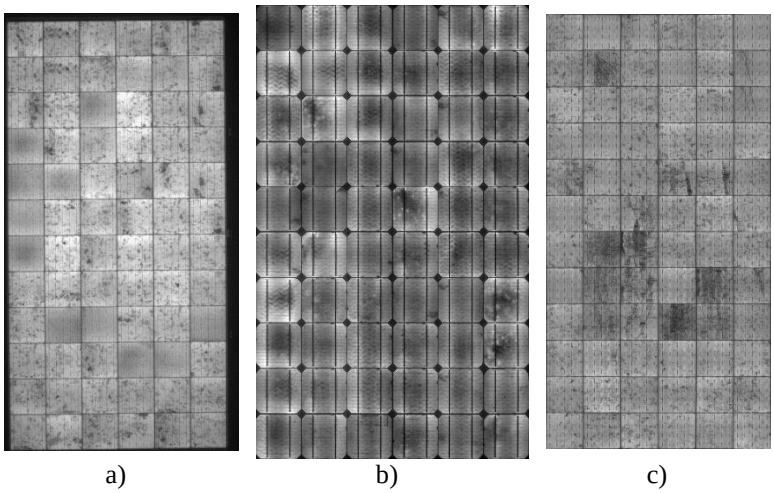

a) b) c)

Fig. 1: a)EL image of a m-Si module imaged in Setup A, b) EL image of a c-Si module imaged in Setup B and c) EL image of a m-Si module imaged in Setup C. All images at 100% Isc.

Figure 2 shows the EL image of a single cell imaged using setup D, in this image the finer details of the image are clearly visible. However, the crack visible in the cell would also be detected in Setup B and C so the value of the additional detail obtained in this image is not necessary for standard quality assessments and should rather be used for research studies.

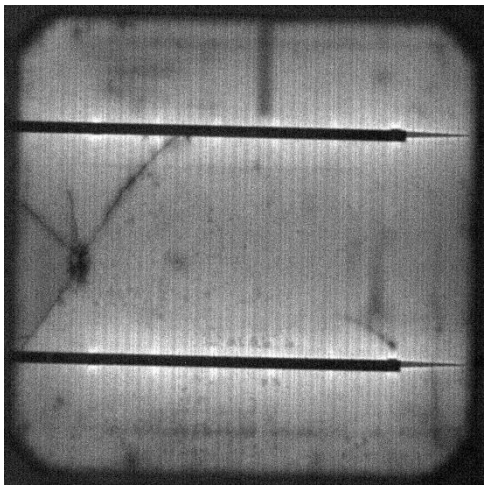

Fig. 2: EL image of a single cell captured using Setup D

Onsite EL can be done on strings in low light conditions setup E. Figure 3, shows an example of the EL of a string of modules taken at low light conditions. This approach can be effective to investigate an array that has been identified by either thermography or the power measurements as having defects. Major defects will be clearly identified in this test, but finer defects will be missed.

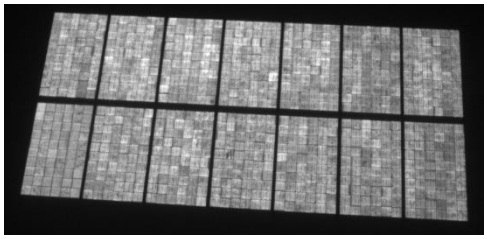

Fig. 3: EL image of an entire module imaged using Setup E.

3.2. Sharpness

The sharpness of the image is affected by the camera focus, lens diffraction and image digitization [9], the limits in sharpness prevent the smallest resolvable object from being the same as the pixel size. IEC TS 60904-13:2018 defines methods for determining the smallest resolvable objects/sharpness and sets defined categories for each sharpness class[5]. In class A, grid fingers are clearly distinguished and the cracks structure is visible. In the class B, grid finger disconnects and cracks that result in a cell disconnect are visible. Class C, the busbars are visible

Class A is optimum for laboratory measurements, Class B is suitable to industrial and quality control measurements and Class C is acceptable for onsite measurements.

Setups D, B and C all achieve sharpness class A, which is due to the module being image in multiple images or with several cameras which contributes to additional cost of equipment or time per measurement.

SETUP	FOV [mm]	Pixel Size [mm]	Image Resolution	Sharpness Class [IEC TS 60904-13:2018]
D	120	0.06	2000	A
B	550	0.27	2048	A
C	2000	0.56	3552	A
A	2100	2.05	1024	B
E	7027	6.86	1024	C

Table 2: EL setups sorted from smallest pixel size to largest, with the Sharpness class as determined by IEC TS 60904-13:2018. The Pixel size is approximate.

4.Conclusions

In order to determine module degradation and compare the quality of different modules the EL images need to be captured in comparable procedures. This paper introduces multiple EL setups and compares the quality of the results obtained. On-site imaging of module strings can only detect major defects and thus is acceptable for onsite inspections. In order to detect micro-cracks and smaller defects it is necessary to image a single

module at a time. The resolution of module imaging can be improved by using more cameras or multiple images, which contributes to the time, cost and processing time of the image. Qualitative assessment of all setups showed major defects were detected but smaller micro-cracks were not detected in the low-resolution imaging setup.

Acknowledgements

The authors gratefully acknowledge the South African Department of Science and Technology (DST), ESKOM, PVinsight (Pty) Ltd, and Nelson Mandela University (NMU) for the financial support and providing necessary facilities for research.

References

[1] Fuyuki, T., H. Kondo, T. Yamazaki, Y. Takahashi, and Y. Uraoka, Photographic surveying of minority carrier diffusion length in polycrystalline silicon solar cells by electroluminescence. Applied Physics Letters, **86**(26) (2005) 262108.

[2] IEAPVPS, Performance and Reliability of Photovoltaic Systems Subtask 3.2:Review of Failures of Photovoltaic Modules, 2014, IEA International Energy Agency.

[3] IEAPVPS, Review on Infrared and Electroluminescence Imaging for PV Field Applications Report IEA-PVPS T13-10:2018, 2018, IEA International Energy Agency.

[4] Crozier, J.L., Photovoltaic Device Characterisation Using Electroluminescence and Other Opto-Electronic Techniques, PhD Thesis, Nelson Mandela Metropolitan University (2015).

[5]"IEC/TS 60904-13Ed.1: Photovoltaic devices -Part 13: Electroluminescence of photovoltaic modules." 2018.

[6] Rau, U., Reciprocity relation between photovoltaic quantum efficiency and electroluminescent emission of solar cells. Physical Review B, 2007. **76**(8).

[7] Potthoff, T., K. Bothe, U. Eitner, D. Hinken, and M. Köntges, Detection of the voltage distribution in photovoltaic modules by electroluminescence imaging. Progress in Photovoltaics: Research and Applications, 2010. **18**(2): p. 100-106.

[8] Wei Luo, Yong Sheng Khoo, Peter Hacke, Volker Naumann, Dominik Lausch, Steven P. Harvey, Jai Prakash Singh, Jing Chai, Yan Wang, Armin G. Aberle, and Seeram Ramakrishna, Energy & Environmental Science **10** (1), 43 (2017).

[9]Bedrich, K., Quantitative Electroluminescence Measurements of PV Devices, PhD Thesis, Loughborough University (2017).

[10]DataArtist, https://github.com/radjkarl/signalToNoise

[11] T. Kirchartz, A. Helbig, and U. Rau, Solar Energy Materials and Solar Cells **92** (12), 1621 (2008).

[12] D. Hinken, C. Schinke, S. Herlufsen, A. Schmidt, K. Bothe, and R. Brendel, Rev Sci Instrum **82** (3), 033706 (2011).